Geophysical Research Letters

RESEARCH LETTER
10.1029/2019GL082367

Key Points:
- Weaker-than-Pinatubo volcanic eruptions with interhemispherically asymmetric forcings can have larger climate impacts than Pinatubo
- Zonal-mean and regional precipitation and TC activity are more sensitive to interhemispherically asymmetric than symmetric eruptions
- Global-mean surface temperature is more sensitive to the NH asymmetric eruptions

Supporting Information:
- Supporting Information S1

Correspondence to:
Wenchang Yang,
wenchang@princeton.edu

Citation:
Yang, W., Vecchi, G., Fueglistaler, S., Horowitz, L. W., Luet, D. J., Muñoz, Á. G., et al. (2019). Climate impacts from large volcanic eruptions in a high-resolution climate model: The importance of forcing structure. *Geophysical Research Letters*, *46*, 7690–7699. https://doi.org/10.1029/2019GL082367

Received 5 FEB 2019
Accepted 12 JUN 2019
Accepted article online 20 JUN 2019
Published online 10 JUL 2019

Climate Impacts From Large Volcanic Eruptions in a High-Resolution Climate Model: The Importance of Forcing Structure

Wenchang Yang[1], Gabriel A. Vecchi[1,2,3], Stephan Fueglistaler[1,2,3], Larry W. Horowitz[4], David J. Luet[1], Ángel G. Muñoz[5], David Paynter[4], and Seth Underwood[4]

[1]Department of Geosciences, Princeton University, Princeton, NJ, USA, [2]Princeton Environmental Institute, Princeton University, Princeton, NJ, USA, [3]Atmospheric and Oceanic Sciences Program, Princeton University, Princeton, NJ, USA, [4]Geophysical Fluid Dynamics Laboratory, NOAA, Princeton, NJ, USA, [5]International Research Institute for Climate and Society, the Earth Institute, Columbia University, Palisades, NY, USA

Abstract Explosivevolcanic eruptions have large climate impacts and can serve as observable tests of the climatic response to radiative forcing. Using a high-resolution climate model, we contrast the climate responses to Pinatubo, with symmetric forcing, and those to Santa Maria and Agung, which had meridionally asymmetric forcing. Although Pinatubo had larger global-mean forcing, asymmetric forcing strongly shifts the latitude of tropical rainfall features, leading to larger local precipitation/tropical cyclone changes. For example, North Atlantic tropical cyclone activity over is enhanced/reduced by SH forcing (Agung)/NH forcing (Santa Maria) but changes little in response to the Pinatubo forcing. Moreover, the transient climate sensitivity estimated from the response to Santa Maria is 20% larger than that from Pinatubo or Agung. This spread in climatic impacts of volcanoes needs to be considered when evaluating the role of volcanoes in global and regional climate and serves to contextualize the well-observed response to Pinatubo.

1. Introduction

Large volcanic eruptions, especially those that occur within low latitudes, can have a great impact on the global climate (Robock, 2000; Swingedouw et al., 2017). Sulfur-rich gases are injected into the stratosphere, where they evolve into sulfate aerosols (Robock, 2000). These aerosols scatter solar radiation, scatter and absorb longwave radiation, and therefore perturb the energy balance of the planet and affect global climate. As a result, global-mean surface temperature decreases while the lower stratosphere warms. These radiative and thermal perturbations can in turn lead to changes in various components of the global climate system, that is, the El Niño–Southern Oscillation (McGregor & Timmermann, 2011; Maher et al., 2015; Stevenson et al., 2016; Khodri et al., 2017; Predybaylo et al., 2017; Liu et al., 2018), the Intertropical Convergence Zone (ITCZ; ; Zuo et al., 2018; Pausata & Camargo, 2019), tropical cyclones or TCs (Evan, 2012; Guevara-Murua et al., 2015; Jones et al., 2017; Yan et al., 2018; Camargo & Polvani, 2019; Pausata & Camargo, 2019), polar vortex and North Atlantic Oscillation (Robock & Mao, 1992; Kirchner et al., 1991; Wunderlich & Mitchell, 2017), Arctic sea ice (Stenchikov et al., 2009; Ding et al., 2014; Gagné et al., 2017), and Atlantic Meridional Overturning Circulation (Stenchikov et al., 2009; Ding et al., 2014; Pausata et al., 2015; Swingedouw et al., 2015). However, the impacts of volcanoes often have large uncertainties that arise either from the low signal-to-noise ratio (Driscoll et al., 2012; Ménégoz et al., 2017; Swingedouw et al., 2017; Wunderlich & Mitchell, 2017; Polvani et al., 2018) or their dependence on the initial state of the climate (Thomas et al., 2009; Zanchettin et al., 2013; Pausata et al., 2015; Swingedouw et al., 2015; Lehner et al., 2016; Pausata et al., 2016; Ménégoz et al., 2017; Gagné et al., 2017; Predybaylo et al., 2017), and the estimation of the impacts might also be model-dependent even the same volcanic radiative properties are specified (Zanchettin et al., 2016).

In addition to the uncertainties described above, climatic impacts from large volcanic eruptions also depend on the latitudinal distribution of stratospheric aerosol loadings and the associated radiative forcing structure (Toohey et al., 2014; Toohey et al., 2019). The volcanic radiative forcing can be approximately balanced between the two hemispheres (symmetric), as in the Pinatubo eruption in 1991, or more concentrated over

a single hemisphere (asymmetric). The differentiated cooling induced by the asymmetric forcing can have important impacts on the climate, especially on the hydroclimate (Haywood et al., 2013; Pausata et al., 2015; Colose et al., 2016). For example, Haywood et al. (2013) found that three of the four driest Sahel summers over the twentieth century were preceded by large NH volcanic eruptions. Using the HadGEM2-ES climate model, they conducted two groups of experiments to compare the Sahel rainfall responses to the NH and SH radiative forcings. In the first group, Sahel rainfall anomaly driven by the El Chichon eruption in 1982, which is a NH-type volcanic forcing (with a 13:6 NH:SH forcing ratio), is compared to that driven by the interhemispherically flipped forcing of El Chichon (and thus is the SH forcing). In the second group, the comparison is between two geoengineering experiments of injecting sulfur dioxide into the stratosphere of NH and SH to mimic the volcanic eruption effect. Both the two groups of experiments indicate an increase (reduction) of Sahel summer rainfall from the SH (NH) volcanic forcing. The Haywood et al. (2013) study was then extended in Jones et al. (2017) to look at TC impacts and they found that North Atlantic TC responds to different types of volcanic forcings in a similar way to the Sahel summer rainfall; that is, SH (NH) volcanic eruptions enhance (reduce) North Atlantic TC activity.

From the numerical experiment in the climate model NorESM1-M to mimic the impact of 1783 Laki eruption in Iceland, Pausata et al. (2015) found that NH high-latitude volcanic eruption pushes the ITCZ southward, weakens the trade winds over the western and central equatorial Pacific, and thus favors a development of an El Niño-like anomaly. They also found that the Atlantic Meridional Overturning Circulation is strengthened in the first 25 years after eruption and then keeps weakening for at least 35 years. Colose et al. (2016) used historical simulations from two climate models (National Aeronautics and Space Administration Goddard Institute for Space Studies ModelE2-R and National Center for Atmospheric Research Community Earth System Model version 1.1) to examine the climatic impact from symmetric and asymmetric volcanic eruptions over the preindustrial part of the last millennium, that is, 850–1850. They also found that the ITCZ shifts away from the hemisphere with greater volcanic forcing. The ITCZ response can be understood in the framework of atmospheric energetics (Kang et al., 2008; Kang et al., 2009; Schneider et al., 2014), which predicts that differentiated heating and cooling between the two hemispheres will push the ITCZ to move from the cooling hemisphere toward the warming hemisphere so that the externally exerted heating and cooling are partly counteracted by the anomalous Hadley circulation.

In this study, we investigate different impacts from symmetric and asymmetric volcanic eruptions by focusing on three of the major explosive volcanic eruptions in the twentieth century: the Pinatubo eruption in 1991 (symmetric), the Agung eruption in 1963 (SH asymmetric), and the Santa Maria eruption in 1902 (NH asymmetric). As a reference, the estimated global stratospheric sulfate loading is 30 Tg for the Pinatubo, 17 Tg for the Agung, and 4 Tg for the Santa Maria (Robock, 2015). We use the Forecast-oriented Low Ocean Resolution (FLOR; Vecchi et al., 2014) coupled climate model to study the impacts from the three eruptions by conducting ensemble perturbation experiments. The FLOR model has a horizontal resolution of about 50 km for the atmosphere and land, which is higher than most models used in the volcanic-eruption-climate modeling and makes it possible for a direct assessment of TC's response to volcanic eruptions. Detailed description of the model is presented below in the subsection of model description. The key questions we will address include the following: How do global surface temperature and precipitation respond differently to the three different types of volcanic eruptions? What is the response of TC activity? Does the climate respond proportionally to the global-mean volcanic forcing? The paper is organized as follows: Section 2 describes the model, experiment setup and volcanic forcing data set. Section 3 presents the results of different climatic impacts from the three eruptions. Conclusions and a discussion are presented in section 4.

2. Methodology

2.1. Model Description

The FLOR model (Vecchi et al., 2014) is a descendant from the CM2.5 (Delworth et al., 2012) and CM2.1 model (Delworth et al., 2006) of the Geophysical Fluid Dynamics Laboratory (GFDL). It keeps the relatively low resolution (approximately 1°) ocean and sea ice components of CM2.1 but has a horizontal resolution of about 50 km in the atmosphere and land, and a significantly improved land model (LM3; Milly et al., 2014) from CM2.5. Thanks to this configuration, the FLOR climate model is capable of resolving TCs directly (i.e., TC permitting) yet is still computationally efficient. It has been extensively used in research of TCs (Vecchi et al., 2014), Arctic sea ice (Msadek et al., 2014), precipitation and temperature over land (Jia et al.,

2015), drought (Delworth et al., 2015), extratropical storms (Yang et al., 2015), the Great Plains Low Level Jet (Krishnamurthy et al., 2015), cross-timescale model diagnostics (Munoz et al., 2017), and the global response to increasing greenhouse gases (Winton et al., 2014). Detailed description and the model code are available from https://www.gfdl.noaa.gov/cm2-5-and-flor website.

2.2. Experiment Setup

The reference experiment for our analysis is a preindustrial control run (without volcanic forcing), where we selected 30 continuous years of simulations (labeled as year 1–30). This period is more than 200 years after the initial year of the control run and the simulated global climate is approximately in equilibrium. Otherwise, we did not set any criteria for the selection of the 30 years. It is expected that the 30 states at the beginning of each year can cover a natural range of initial conditions for the 30-ensemble volcanic perturbation simulations, where historical volcanic forcings are introduced in model integration. Besides this additional volcanic forcing, all other radiative forcings are kept at the same level as in the preindustrial control run. Each member of the perturbation simulations is integrated forward for 5 years and is compared to the corresponding 5-year control run. Taking the Agung volcanic experiment, for example, the first member perturbation simulation starts from the initial state of the year 1 from the control run and is forced by historical volcanic forcings of years 1963–1967 during the 5-year integration. The 5-year perturbation simulation is then compared to year 1–5 of the control run and the difference is defined as the volcanic impact. Similarly, the nth member perturbation simulation is compared to the segment of the control run from year n to $n+4$ ($n = 1, 2, \ldots, 30$).

To estimate the radiative forcing at top of atmosphere from each volcanic experiment during the 5 years, we also conduct a series of "nudged" experiments, where the sea surface temperature and salinity are nudged to the climatology of the preindustrial fully coupled control run. The nudged perturbation experiments for the three volcanoes are performed in a similar way to the fully coupled ones, but only 10 ensemble simulations are applied. The ensemble mean difference of the net radiation at top of atmosphere between the nudged control run and the nudged perturbation run is used to represent the radiative forcing from each of the three volcanic eruptions.

2.3. Historical Volcanic Forcing Data Set

The historical volcanic forcing is from the Coupled Model Intercomparison Project Phase 6 stratospheric aerosol data set and includes: version 3 of extinction coefficients for both shortwave and longwave radiation, and version 4 of single scattering albedo and asymmetrical factors only for the shortwave radiation. While the data over the period of 1979–2014 are based on satellite observations (Thomason et al., 2018), they are generally calculated using the AER2D model over the period of 1850–1978 (Arfeuille et al., 2014). Detailed description of the volcanic aerosol data is available from ftp://iacftp.ethz.ch/pub_read/luo/CMIP6/Readme_Data_Description.pdf website. The extinction coefficients for the shortwave radiation at the mid-visible bandwidth (550 nm) summed vertically is shown in Figure S1 in the supporting information as a function of time and latitude. The difference in the latitudinal distribution from the three volcanic eruptions are apparent from the figure.

3. Results

3.1. Global-/Hemispheric-Mean Time Series

Figure 1 shows the global-/hemispheric-mean time series of volcanic radiative forcings and impacts from the three eruptions. The global-mean volcanic forcing from Pinatubo has the largest magnitude and reaches its maximum of about -3 W/m^2 near the end of the eruption year, much the same as that reported in the GFDL CM2.1 model (Merlis et al., 2014). After that, the forcing returns to the near-zero level in years 4 and 5. The hemispheric mean aerosol forcing from the Pinatubo eruption shows variations on annual time scale, which arise from the effect that solar radiation is scattered more in the summer than winter hemisphere given the same amount of volcanic aerosols in each hemisphere. Besides that, the Pinatubo forcing has little difference between the SH and NH. However, the response of surface temperature (T_s) does have a contrast between SH and NH (Figure 1d), largely due to the difference in land area fraction between the two hemispheres. The interhemispheric difference of surface temperature reaches its maximum in year 2 and can be as large as 0.3 K.

The relationship between volcanic forcing and surface temperature response differs for the eruption of Agung in 1963. While the global-mean forcing (Figure 1b) is weaker than that of Pinatubo, with the maxi-

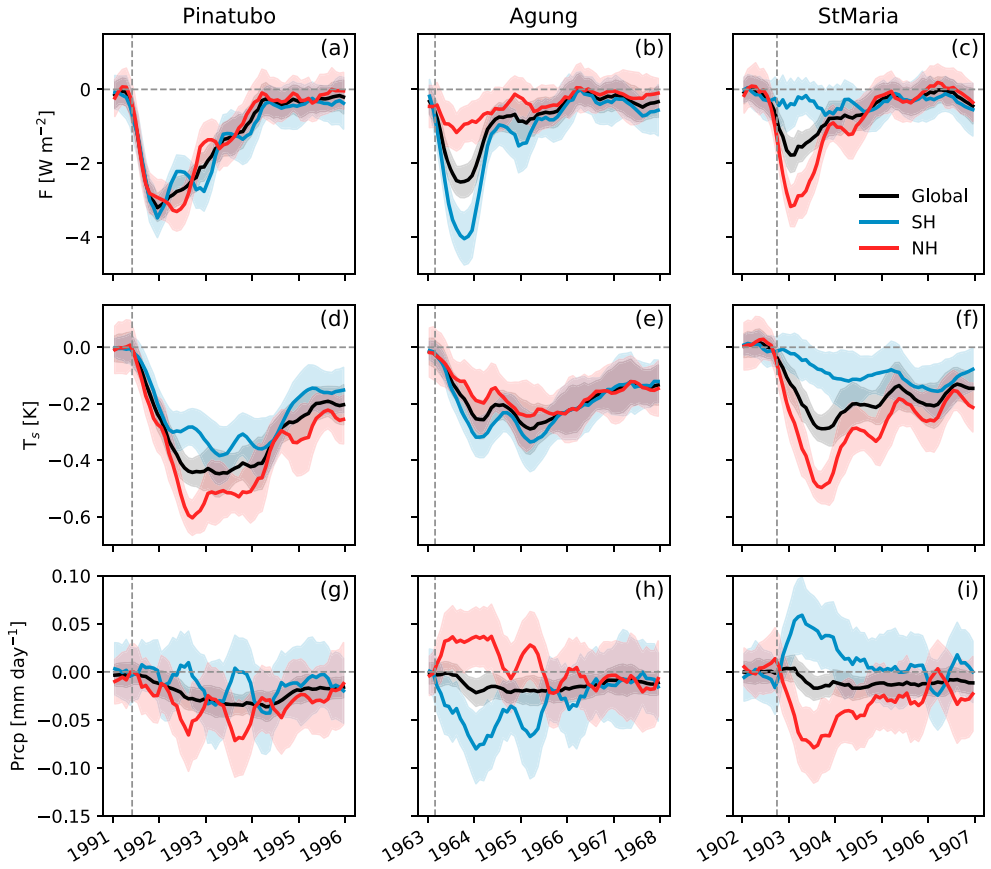

Figure 1. Volcanic forcing (a–c), responses of surface temperature (d–f), and precipitation rate (g–i) averaged globally (black), southern hemispherically (blue), and northern hemispherically (red) for the three volcanic eruptions of Pinatubo (left column), Agung (middle column), and Santa Maria (right column). Lines are the ensemble means while shadings represent 95% confidence intervals of the ensemble means. All the quantities are smoothed by a 5-month running average.

mum value around −2.5 W/m^2, the forcing is much stronger in the SH than NH and exceeds that of Pinatubo in the SH. The forcing contrast between the SH and NH can be as large as 3 W/m^2. Due to the strong interhemispheric differentiated cooling, the response of surface temperature from Agung is larger in the SH than NH (Figure 1e), which is just opposite to that of the Pinatubo case. Relative to Pinatubo, Agung has a comparable surface temperature response in the SH but a much weaker response in the NH. As a result, the global-mean surface temperature response is weaker from Agung than Pinatubo.

The eruption from Santa Maria has an opposite meridional forcing structure compared to Agung, with stronger forcing in the NH (Figure 1c). Driven by both the forcing structure and the land-area-fraction effect, the surface temperature response for Santa Maria is much larger in the NH (0.5 K) than SH (0.1 K). The NH response from Santa Maria is stronger than both the global/hemispheric means from Agung and the global/SH means from Pinatubo, and only weaker than the Pinatubo NH mean.

Similar to the surface temperature response, the precipitation response is also largest in the Pinatubo eruption in terms of global mean. However, unlike for surface temperature, the precipitation response over the eruption hemisphere is substantially larger in the two asymmetric volcanic eruptions of Agung and Santa Maria than in Pinatubo, as shown in Figures 1g–1i. In addition, the interhemispheric contrast is also larger for Agung and Santa Maria than Pinatubo. The precipitation response over the hemisphere away from the eruption is positive in general for the two asymmetric eruptions. Therefore, the two asymmetric volcanic eruptions do have a stronger hydroclimate response hemispherically, although the response in terms of global mean is smaller than that of Pinatubo.

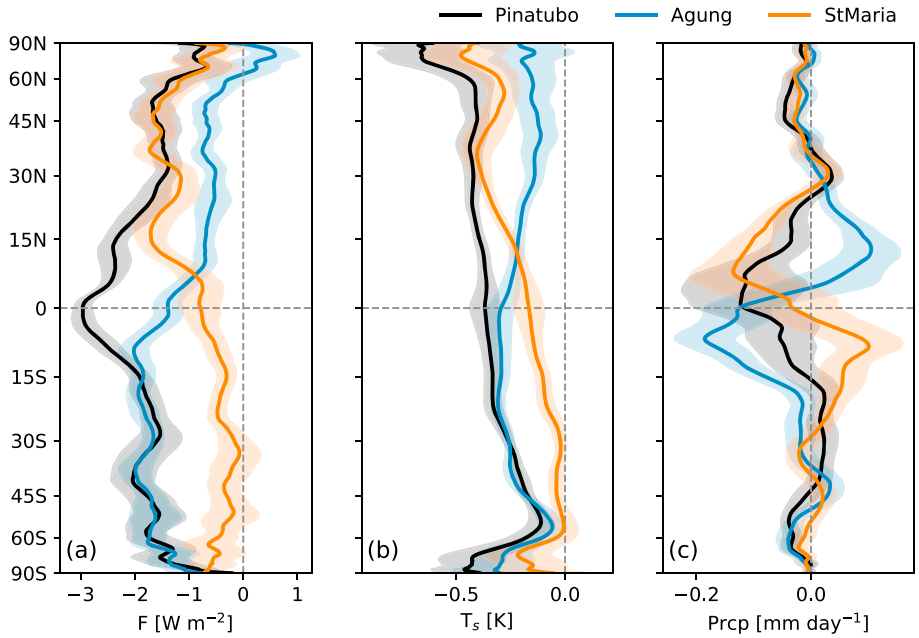

Figure 2. Time-and-zonal-mean volcanic forcing (a), surface temperature (b), and precipitation rate (c) for Pinatubo (black), Agung (blue), and Santa Maria (orange). Lines are the ensemble means while shadings represent 95% confidence intervals of the ensemble means. The time-mean is over the 3 years following the eruption (i.e., June 1991 to May 1994 for Pinatubo, March 1963 to February 1966 for the Agung, and October 1902 to September 1905 for the Santa Maria). All the quantities are smoothed by a nine-point (of 0.5° model grid cells) running average along the meridional dimension.

3.2. Zonal Mean Forcing and Responses

Figure 2 shows the zonal-mean forcings and impacts averaged over the three years following the eruption. The forcing from Pinatubo is approximately symmetric between the two hemispheres, with the highest level of about −3 W/m^2 near the equator. The forcing from Agung is almost identical to that from Pinatubo from 90°S to 15°S but starts to weaken further north. In contrast, the forcing from Santa Maria is comparable to Pinatubo from 90°N to 30°N but weakens further south.

Due to the interhemispherically asymmetric cooling, the responses of surface temperature from Agung and Santa Maria also show a contrast between the two hemispheres. While the response over high latitudes of the eruption hemisphere is comparable to or slightly weaker than that from Pinatubo, it is much weaker over the other hemisphere and even close to zero (e.g., 30–60°S for Santa Maria). An interesting aspect of the surface temperature response is that the ensemble spread is larger over the extratropics than the tropics and peaks near the polar latitudes. This might be related to large internal variability due to synoptic weather systems over the extratropics and ice albedo feedbacks over the polar regions. The response of precipitation has a different latitudinal distribution from surface temperature. In general, the Pinatubo eruption reduces precipitation strongly in the tropics and slightly over high latitudes but strengthens precipitation in the subtropics, somewhat opposite to the "wet-get-wetter" impact of greenhouse gases induced global warming (Held & Soden, 2006). The two asymmetric volcanoes, however, have a different pattern from that of Pinatubo. They both greatly reduce precipitation over the higher aerosol loading hemisphere and enhance precipitation over the other hemisphere, in both the tropics and subtropics. The amplitudes of the response are also comparable to or even larger than that of Pinatubo. Therefore, Agung and Santa Maria can have a higher impact on the hydroclimate than Pinatubo, although they have a weaker global-mean forcing or global-mean surface temperature response.

3.3. TC Response

The high resolution of the FLOR model and its good performance in TC simulation and prediction (Vecchi et al., 2014; Murakami et al., 2016; Zhang et al., 2018) encourage a direct assessment of the TC responses to the three volcanic eruptions. The zonal-mean TC density response averaged over the three years following the eruption (Figures 3a, 3c, and 3e) peaks at around 15° latitude in both hemispheres, where the climatology

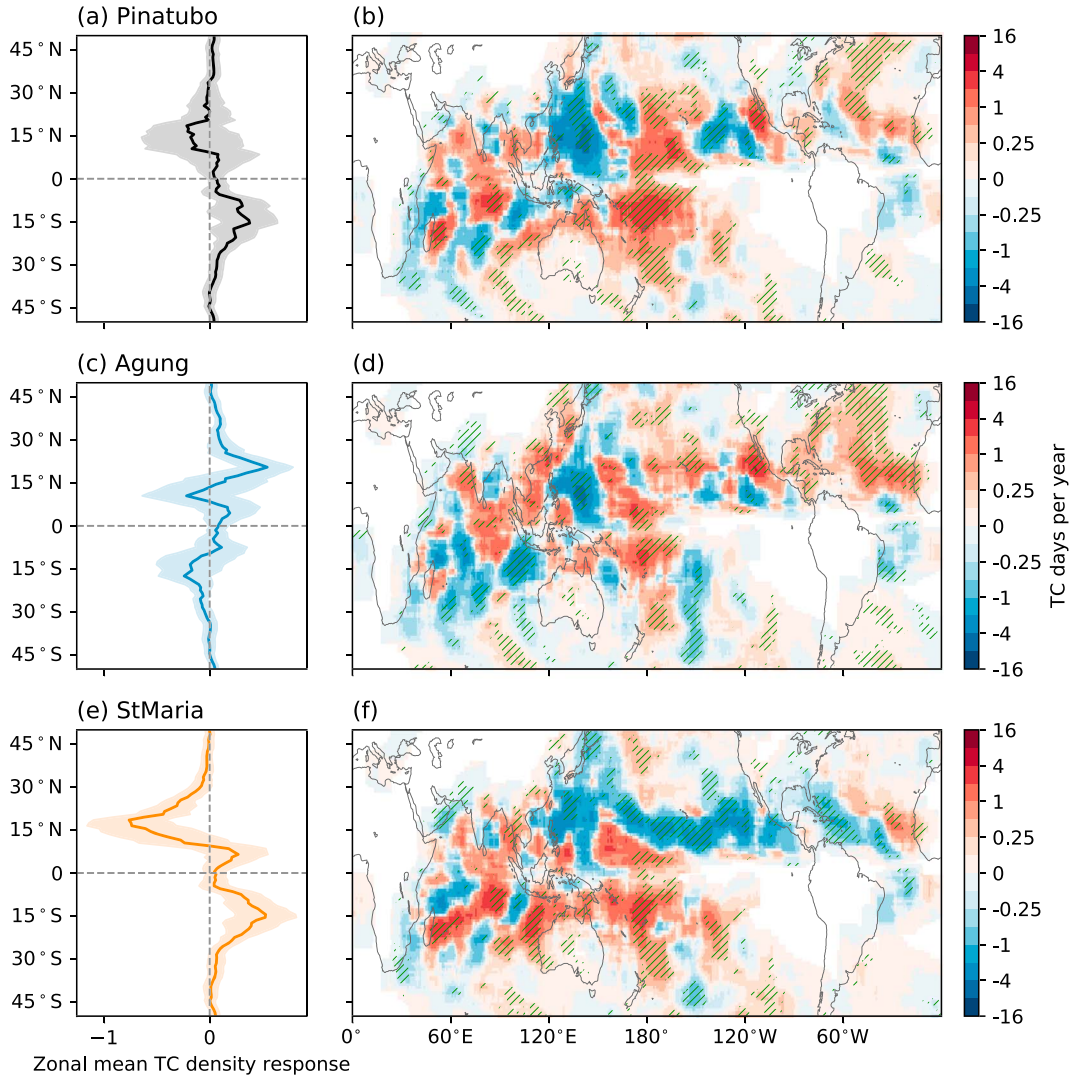

Figure 3. Response of TC density to the eruption of Pinatubo (a, b), Agung (c, d), and Santa Maria (e, f). The TC density is defined as the total TC track duration (in days) per year within a 10° × 10° grid box centered on each of the global 1° × 1° grid boxes. The right column shows the maps of TC density response averaged over the 3 years following the eruption (i.e., June 1991 to May 1994 for Pinatubo, March 1963 to February 1966 for Agung, and October 1902 to September 1905 for Santa Maria), where hatched areas indicate significant values at the 0.05 level by the two-sided Student's *t* test. The left column shows the zonal mean values of the right column (lines) as well as the 95% confidence interval (shading).

of the control run also peaks (Figure S3). Although the Pinatubo is the largest eruption among the three volcanoes, its zonal-mean TC response (Figure 3a) has the smallest amplitude and is only slightly reduced (increased) in the NH (SH). Agung (Figure 3c) and Santa Maria (Figure 3e) have a much larger TC response. Quantitatively, the peak responses from the Santa Maria in both hemispheres and from the Agung in the NH are about 10% of the control climatology (Figures S3 and S6). In both cases, the TC density is reduced in the larger forcing hemisphere but enhanced in the other hemisphere, similar to the precipitation and ITCZ response seen in Figure 2c.

The global maps of TC density response (Figures 3b, 3d, and 3f) show some noise but still distinctive features from the three volcanoes. For example, TC density over the East Pacific basin is in general enhanced from Agung (Figure 3d) but reduced in most grid boxes from the Santa Maria (Figure 3f), and both enhanced and reduced TC densities are seen from the Pinatubo (Figure 3b). Another interesting basin is the North Atlantic, where different responses of TC density from the three volcanoes are most apparent (Figure S5). Pinatubo has the weakest response, with positive and negative values almost evenly distributed over the basin. In

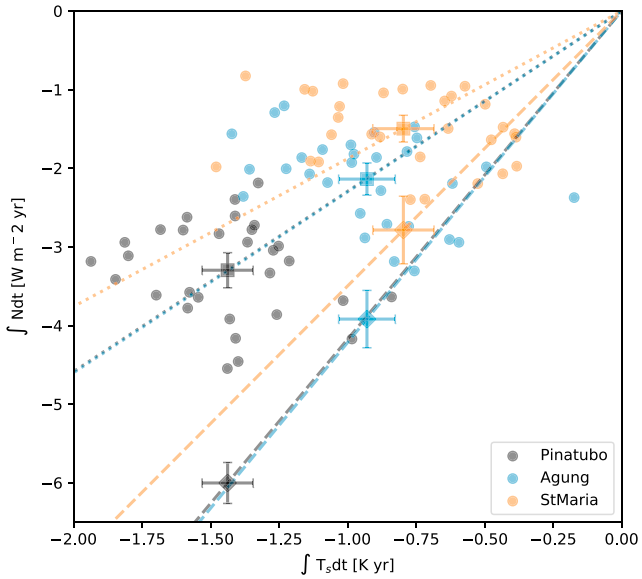

Figure 4. Scatter plot of top of atmosphere net radiation versus surface temperature anomalies integrated over the 5 years of simulation. The filled circles represent each individual ensemble member. The squares are the ensemble means. The diamonds share the same surface temperature as the squares but the top of atmosphere net radiation values come from the nudged experiments and thus represent the radiative forcings from the volcanic eruptions. Error bars indicate 95% confidence intervals of the ensemble means. The dotted/dashed lines link the origin and the points of squares/diamonds.

contrast, the Agung and Santa Maria drive a stronger response and show a clear overall TC increase and decrease, respectively. Quantitatively, the basin-mean TC density increase (decrease) from Agung (Santa Maria) can be as much as 30% of the climatology over the first 2 years since the eruption (Figure S5a). These results are in general consistent with genesis potential index, or GPI (Emanuel & Nolan, 2004), response to volcanic forcing in these experiments (Figure S7). Decomposition of the GPI reveals that components of relative humidity, potential intensity, and vertical wind shear all contribute substantially to the overall GPI change, while the contribution from the vorticity component is secondary (Figures S8–S11). This importance of shear, potential intensity and humidity bears resemblance to modeled GPI response to CO_2 increase (Vecchi & Soden, 2007).

3.4. Transient Climate Sensitivity

The three volcanoes also show different properties of transient climate sensitivity and ocean heat uptake efficiency, which is of interest to studies using volcanic eruptions to constrain transient climate sensitivity (Merlis et al., 2014). Transient climate sensitivity is defined here as the 5-year integrated global-mean surface temperature divided by the integrated global-mean radiative forcing (Merlis et al., 2014), which is inversely proportional to the slope of the dashed lines in Figure 4. While the case of Agung has a slightly larger slope than Pinatubo and thus a slightly lower transient climate sensitivity, the Santa Maria has a distinctively smaller slope and thus a larger transient climate sensitivity (about 20%). This difference might be related to the interaction of the land-fraction effect and the disparity of the volcanic forcing distribution. Ocean heat uptake efficiency (Winton et al., 2010; He et al., 2017) also contributes, at least partly, to the unique transient climate sensitivity from the Santa Maria experiment, as indicated by the slopes of the dotted lines.

4. Conclusions and Discussion

Some recent studies have noted the importance of forcing structure in the climatic impact from large volcanic eruptions (Haywood et al., 2013; Pausata et al., 2015; Colose et al., 2016). Here we compare the impacts from three explosive volcanic eruptions in the twentieth century that have different radiative forcing structures, including the Pinatubo eruption in 1991 (interhemispherically symmetric), the Agung eruption in 1963 (asymmetric and SH dominant), and the Santa Maria eruption in 1902 (asymmetric and NH dominant). By conducting a suite of 5-year ensemble perturbation experiments using the high-resolution TC-permitting FLOR climate model, we find the following:

- The mean responses of surface temperature in the higher aerosol loading hemisphere from Agung and Santa Maria are comparable to that from Pinatubo, although the magnitudes of the two asymmetric eruptions are much smaller than that of Pinatubo in terms of global-mean forcing or global-mean surface temperature response.
- The hemispheric mean precipitation responses are larger from the Agung and Santa Maria eruptions than the Pinatubo and imply a shift of ITCZ away from the higher stratospheric aerosol forcing hemisphere that is consistent with previous studies.
- The Agung and Santa Maria eruptions also have a stronger impact on TC activity than Pinatubo and shift the TC activity away from the large forcing hemisphere. The TC activity response has the most apparent differences over the North Atlantic basin from the three eruptions.
- The global-mean surface temperature does not respond proportionally to the forcings from the three eruptions. The Santa Maria has the largest sensitivity, while the sensitivity from the other two eruptions are almost identical.

Since its eruption in 1991, the Pinatubo has drawn much more attention in the study of climatic impact from volcanoes, in large part because it is the largest eruption in the twentieth century and better observed

than previous eruptions. Pinatubo has been used as a typical example of how an explosive volcanic eruption can impact the climate (Robock, 2013). Other eruptions in the twentieth century are often assumed to have a weaker impact (Driscoll et al., 2012). We demonstrate that these smaller eruptions can also have larger impact, especially on hemispheric regional precipitation and TC activity, inducing an ITCZ shift larger than that induced by Pinatubo. These results highlight the importance of volcanic forcing spatial structure on its climatic impact, which has consequential implications on our understanding and interpretations of the climate in the past or in the future projections.

Most of current climate models do not couple volcanic aerosols directly but rather incorporate their radiative properties (e.g., extinction coefficient and scatter parameters) in a passive way, which in turn are generally calculated using stratospheric microphysics/transport models that assimilate limited observed proxies if no direct satellite observations are available (Sato et al., 1993; Stenchikov et al., 1998; Ammann et al., 2003; Gao et al., 2008; Crowley & Unterman, 2013; Toohey et al., 2016). Our findings indicate that it is crucial to obtain an accurate reconstruction of volcanic aerosol radiative property spatial structure in order to get a correct impact in climate modeling, especially for the hydroclimate. We should take this kind of uncertainty into consideration when interpreting climate model output that forced by historical volcanic eruptions, for example, Coupled Model Intercomparison Project Phase 5 (Taylor et al., 2012) historical runs or the Community Earth System Model-Last Millennium Ensemble modeling project (Otto-Bliesner et al., 2016).

Acknowledgments
This work is supported by NOAA/OCO (NA18OAR4310418), NOAA/MAPP (NA18OAR4310273), the Carbon Mitigation Initiative (CMI), and the Cooperative Institute for Modeling the Earth System (CIMES; NA18OAR4320123) at Princeton University. The simulations presented in this article were performed on computational resources managed and supported by Princeton Research Computing, a consortium of groups including the Princeton Institute for Computational Science and Engineering (PICSciE) and the Office of Information Technology's High Performance Computing Center and Visualization Laboratory at Princeton University. The source code for the model used in this study, the GFDL/CM2.5(FLOR), is freely available at https://www.gfdl.noaa.gov/cm2-5-and-flor website . The data and scripts used in our analyses are available from http://tigress-web.princeton.edu/~wenchang/pub/GRL2019Volcanic/data and https://github.com/wy2136/GRL2019Volcanic websites, respectively.

References

Ammann, C. M., Meehl, G. A., Washington, W. M., & Zender, C. S. (2003). A monthly and latitudinally varying volcanic forcing dataset in simulations of 20th century climate. *Geophysical Research Letters*, *30*(12), 1657. https://doi.org/10.1029/2003GL016875

Arfeuille, F., Weisenstein, D., Mack, H., Rozanov, E., Peter, T., & Brnnimann, S. (2014). Volcanic forcing for climate modeling: A new microphysics-based data set covering years 1600–present. *Climate of the Past*, *10*(1), 359–375. https://doi.org/10.5194/cp-10-359-2014

Camargo, S. J., & Polvani, L. M. (2019). Little evidence of reduced global tropical cyclone activity following recent volcanic eruptions. *npj Climate and Atmo-spheric Science*, *2*(1). https://doi.org/10.1038/s41612-019-0070-z

Colose, C. M., LeGrande, A. N., & Vuille, M. (2016). Hemispherically asymmetric volcanic forcing of tropical hydroclimate during the last millennium. *Earth System Dynamics*, *7*(3), 681–696. https://doi.org/10.5194/esd-7-681-2016

Crowley, T. J., & Unterman, M. B. (2013). Technical details concerning development of a 1200 yr proxy index for global volcanism. *Earth System Science Data*, *5*(1), 187–197. https://doi.org/10.5194/essd-5-187-2013

Delworth, T. L., Broccoli, A. J., Rosati, A., Stouffer, R. J., Balaji, V., Beesley, J. A., & Zhang, R. (2006). GFDL's CM2 global coupled climate models. Part I: Formulation and simulation characteristics. *Journal of Climate*, *19*(5), 643–674. https://doi.org/10.1175/jcli3629.1

Delworth, T. L., Rosati, A., Anderson, W., Adcroft, A. J., Balaji, V., Benson, R., & Zhang, R. (2012). Simulated climate and climate change in the GFDL CM2.5 high-resolution coupled climate model. *Journal of Climate*, *25*(8), 2755–2781. https://doi.org/10.1175/jcli-d-11-00316.1

Delworth, T. L., Zeng, F., Rosati, A., Vecchi, G. A., & Wittenberg, A. T. (2015). A link between the hiatus in global warming and North American drought. *Journal of Climate*, *28*(9), 3834–3845. https://doi.org/10.1175/jcli-d-14-00616.1

Ding, Y., Carton, J. A., Chepurin, G. A., Stenchikov, G., Robock, A., Sentman, L. T., & Krasting, J. P. (2014). Ocean response to volcanic eruptions in Coupled Model Intercomparison Project 5 simulations. *Journal of Geophysical Research: Oceans*, *119*, 5622–5637. https://doi.org/10.1002/2013jc009780

Driscoll, S., Bozzo, A., Gray, L. J., Robock, A., & Stenchikov, G. (2012). Coupled Model Intercomparison Project 5 (CMIP5) simulations of climate following volcanic eruptions. *Journal of Geophysical Research*, *117*, D17105. https://doi.org/10.1029/2012JD017607

Emanuel, K., & Nolan, D. (2004). Tropical cyclone activity and the global climate system. In *26th conference on hurricanes and tropical meteorology* (pp. 240–241).

Evan, A. T. (2012). Atlantic hurricane activity following two major volcanic eruptions. *Journal of Geophysical Research*, *117*, D06101. https://doi.org/10.1029/2011JD016716

Gagnė, M.-È., Kirchmeier-Young, M. C., Gillett, N. P., & Fyfe, J. C. (2017). Arctic sea ice response to the eruptions of Agung El Chichon, and Pinatubo. *Journal of Geophysical Research: Atmospheres*, *122*, 8071–8078. https://doi.org/10.1002/2017jd027038

Gao, C., Robock, A., & Ammann, C. (2008). Volcanic forcing of climate over the past 1500 years: An improved ice core-based index for climate models. *Journal of Geophysical Research*, *113*, D23111. https://doi.org/10.1029/2008JD010239

Guevara-Murua, A., Hendy, E. J., Rust, A. C., & Cashman, K. V. (2015). Consistent decrease in North Atlantic tropical cyclone frequency following major volcanic eruptions in the last three centuries. *Geophysical Research Letters*, *42*, 9425–9432. https://doi.org/10.1002/2015gl066154

Haywood, J. M., Jones, A., Bellouin, N., & Stephenson, D. (2013). Asymmetric forcing from stratospheric aerosols impacts Sahelian rainfall. *Nature Climate Change*, *3*(7), 660–665. https://doi.org/10.1038/nclimate1857

He, J., Winton, M., Vecchi, G., Jia, L., & Rugenstein, M. (2017). Transient climate sensitivity depends on base climate ocean circulation. *Journal of Climate*, *30*(4), 1493–1504. https://doi.org/10.1175/jcli-d-16-0581.1

Held, I. M., & Soden, B. J. (2006). Robust responses of the hydrological cycle to global warming. *Journal of Climate*, *19*(21), 5686–5699. https://doi.org/10.1175/JCLI3990.1

Jia, L., Yang, X., Vecchi, G. A., Gudgel, R. G., Delworth, T. L., Rosati, A., & Dixon, K. (2015). Improved seasonal prediction of temperature and precipitation over land in a high-resolution GFDL climate model. *Journal of Climate*, *28*(5), 2044–2062. https://doi.org/10.1175/jcli-d-14-00112.1

Jones, A. C., Haywood, J. M., Dunstone, N., Emanuel, K., Hawcroft, M. K., Hodges, K. I., & Jones, A. (2017). Impacts of hemispheric solar geoengineering on tropical cyclone frequency. *Nature Communications*, *8*(1), 1382. https://doi.org/10.1038/s41467-017-01606-0

Kang, S. M., Frierson, D. M. W., & Held, I. M. (2009). The tropical response to extratropical thermal forcing in an idealized GCM: The importance of radiative feedbacks and convective parameterization. *Journal of the Atmospheric Sciences*, *66*(9), 2812–2827. https://doi.org/10.1175/2009jas2924.1

Kang, S. M., Held, I. M., Frierson, D. M. W., & Zhao, M. (2008). *Journal of Climate*, *21*(14), 3521–3532. https://doi.org/10.1175/2007jcli2146.1

Khodri, M., Izumo, T., Vialard, J., Janicot, S., Cassou, C., Lengaigne, M., & McPhaden, M. J. (2017). Tropical explosive volcanic eruptions can trigger El Niño by cooling tropical Africa. *Nature Communications*, *8*(1). https://doi.org/10.1038/s41467-017-00755-6

Kirchner, I., Stenchikov, G. L., Graf, H.-F., Robock, A., & na, Antu (1991). J. C. (1999). Climate model simulation of winter warming and summer cooling following the Mount Pinatubo volcanic eruption. *Journal of Geophysical Research*, *104*(D16), 19,039–19,055. https://doi.org/10.1029/1999JD900213

Krishnamurthy, L., Vecchi, G. A., Msadek, R., Wittenberg, A., Delworth, T. L., & Zeng, F. (2015). The seasonality of the Great Plains low-level jet and ENSO relationship. *Journal of Climate*, *28*(11), 4525–4544. https://doi.org/10.1175/jcli-d-14-00590.1

Lehner, F., Schurer, A. P., Hegerl, G. C., Deser, C., & Frlicher, T. L. (2016). The importance of ENSO phase during volcanic eruptions for detection and attribution. *Geophysical Research Letters*, *43*, 2851–2858. https://doi.org/10.1002/2016gl067935

Liu, F., Li, J., Wang, B., Liu, J., Li, T., Huang, G., & Wang, Z. (2018). Divergent El Niño responses to volcanic eruptions at different latitudes over the past millennium. *Climate Dynamics*, *50*(9-10), 3799–3812. https://doi.org/10.1007/s00382-017-3846-z

Maher, N., McGregor, S., England, M. H., & Gupta, A. S. (2015). Effects of volcanism on tropical variability. *Geophysical Research Letters*, *42*, 6024–6033. https://doi.org/10.1002/2015gl064751

McGregor, S., & Timmermann, A. (2011). The effect of explosive tropical volcanism on ENSO. *Journal of Climate*, *24*(8), 2178–2191. https://doi.org/10.1175/2010jcli3990.1

Ménégoz, M., Cassou, C., Swingedouw, D., & Ruprich-Robert, Y. (2017). *BretonniÈre*. P.-A., and Doblas-Reyes, F: Role of the Atlantic multidecadal variability in modulating the climate response to a Pinatubo-like volcanic eruption. Climate Dynamics. https://doi.org/10.1007/s00382-017-3986-1

Merlis, T. M., Held, I. M., Stenchikov, G. L., Zeng, F., & Horowitz, L. W. (2014). Constraining transient climate sensitivity using coupled climate model simulations of volcanic eruptions. *Journal of Climate*, *27*(20), 7781–7795. https://doi.org/10.1175/jcli-d-14-00214.1

Milly, P. C. D., Malyshev, S. L., Shevliakova, E., Dunne, K. A., Findell, K. L., & Gleeson, T. (2014). Swenson, s. *An enhanced model of land water and energy for global hydrologic and Earth-system studies. Journal of Hydrometeorology*, *15*(5), 1739–1761. https://doi.org/10.1175/jhm-d-13-0162.1

Msadek, R., Vecchi, G. A., Winton, M., & Gudgel, R. G. (2014). Importance of initial conditions in seasonal predictions of Arctic sea ice extent. *Geophysical Research Letters*, *41*, 5208–5215. https://doi.org/10.1002/2014gl060799

Munoz, G., Vecchi, G. A., Robertson, A. W., & Cooke, W. F. (2017). A weather-type-based cross-time-scale diagnostic framework for coupled circulation models. *Journal of Climate*, *30*(22), 8951–8972. https://doi.org/10.1175/JCLI-D-17-0115.1

Murakami, H., Villarini, G., Vecchi, G. A., Zhang, W., & Gudgel, R. (2016). Statisticaldynamical seasonal forecast of North Atlantic and U.S. landfalling tropical cyclones using the high-resolution GFDL FLOR coupled model. *Monthly Weather Review*, *144*(6), 2101–2123. https://doi.org/10.1175/MWR-D-15-0308.1

Otto-Bliesner, B. L., Brady, E. C., Fasullo, J., Jahn, A., Landrum, L., & Stevenson, S. (2016). Strand, g. *Climate variability and change since 850 CE: An ensemble approach with the Community Earth System Model. Bulletin of the American Meteorological Society*, *97*(5), 735–754. https://doi.org/10.1175/bams-d-14-00233.1

Pausata, F. S. R., & Camargo, S. J. (2019). Tropical cyclone activity affected by volcanically induced ITCZ shifts. *Proceedings of the National Academy of Sciences of the United States of America*, *116*(16), 7732–7737. https://doi.org/10.1073/pnas.1900777116

Pausata, F. S. R., Chafik, L., Caballero, R., & Battisti, D. S. (2015). Impacts of high-latitude volcanic eruptions on ENSO and AMOC. *Proceedings of the National Academy of Sciences of the United States of America*, *112*(45), 13,784–13,788. https://doi.org/10.1073/pnas.1509153112

Pausata, F. S. R., Grini, A., Caballero, R., & Hannachi, A. (2015). Seland High latitude volcanic eruptions in the Norwegian Earth System Model: the effect of different initial conditions and of the ensemble size. *Tellus B: Chemical and Physical Meteorology*, *67*(1), 26728. https://doi.org/10.3402/tellusb.v67.26728

Pausata, F. S. R., Karamperidou, C., Caballero, R., & Battisti, D. S. (2016). ENSO Response to high-latitude volcanic eruptions in the Northern Hemisphere: The role of the initial conditions. *Geophysical Research Letters*, *43*, 8694–8702. https://doi.org/10.1002/2016GL069575

Polvani, L. M., Banerjee, A., & Schmidt, A. (2018). Northern hemisphere continental winter warming following the 1991 Mt. Pinatubo eruption: Reconciling models and observations. *Atmospheric Chemistry and Physics Discussions*, 1–25. https://doi.org/10.5194/acp-2018-333

Predybaylo, E., Stenchikov, G. L., Wittenberg, A. T., & Zeng, F. (2017). Impacts of a Pinatubo-size volcanic eruption on ENSO. *Journal of Geophysical Research: Atmospheres*, *122*, 925–947. https://doi.org/10.1002/2016jd025796

Robock, A. (2000). Volcanic eruptions and climate. *Reviews of Geophysics*, *38*(2), 191–219. https://doi.org/10.1029/1998RG000054

Robock, A. (2013). Introduction: Mount Pinatubo as a test of climate feedback mechanisms. In Volcanism and the Earth's atmosphere, *American Geophysical Union (AGU)*. https://doi.org/10.1029/139GM01

Robock, A. (2015). Chapter 53—Climatic impacts of volcanic eruptions. In H. Sigurdsson (Ed.), *The encyclopedia of volcanoes* (2nd ed., pp. 935–942). Amsterdam: Academic Press. https://doi.org/10.1016/B978-0-12-385938-9.00053-5

Robock, A., & Mao, J. (1992). Winter warming from large volcanic eruptions. *Geo-physical Research Letters*, *19*(24), 2405–2408. https://doi.org/10.1029/92GL02627

Sato, M., Hansen, J. E., McCormick, M. P., & Pollack, J. B. (1993). Stratospheric aerosol optical depths 18501990. *Journal of Geophysical Research*, *98*(D12), 22987. https://doi.org/10.1029/93JD02553

Schneider, T., Bischoff, T., & Haug, G. H. (2014). Migrations and dynamics of the Intertropical Convergence Zone. *Nature*, *513*, 45–53. https://doi.org/10.1038/nature13636

Stenchikov, G., Delworth, T. L., Ramaswamy, V., Stouffer, R. J., Wittenberg, A., & Zeng, F. (2009). Volcanic signals in oceans. *Journal of Geophysical Research*, *114*. https://doi.org/10.1029/2008JD011673

Stenchikov, G., Kirchner, I., Robock, A., Graf, H.-F., Antu na, J. C., Grainger, R. G., & Thomason, L. (1998). Radiative forcing from the 1991 Mount Pinatubo volcanic eruption. *Journal of Geophysical Research*, *103*, 13,837–13,857. https://doi.org/10.1029/98JD00693

Stevenson, S., Otto-Bliesner, B., Fasullo, J., & Brady, E. (2016). El Niño like hydroclimate responses to last millennium volcanic eruptions. *Journal of Climate*, *29*(8), 2907–2921. https://doi.org/10.1175/JCLI-D-15-0239.1

Swingedouw, D., Mignot, J., Ortega, P., Khodri, M., Menegoz, M., Cassou, C., & Hanquiez, V. (2017). Impact of explosive volcanic eruptions on the main climate variability modes. *Global and Planetary Change, 150*, 24–45. https://doi.org/10.1016/j.gloplacha.2017.01.006

Swingedouw, D., Ortega, P., Mignot, J., Guilyardi, E., Masson-Delmotte, V., & Butler, P. G. (2015). Séférian, R Bidecadal North Atlantic ocean circulation variability controlled by timing of volcanic eruptions. *Nature Communications*, *6*(1). https://doi.org/10.1038/ncomms7545

Taylor, K. E., Stouffer, R. J., & Meehl, G. A. (2012). An overview of CMIP5 and the experiment design. *Bulletin of the American Meteorological Society*, *93*(4), 485–498. https://doi.org/10.1175/BAMS-D-11-00094.1

Thomas, M. A., Timmreck, C., Giorgetta, M. A., Graf, H.-F., & Stenchikov, G. (2009). Simulation of the climate impact of Mt. Pinatubo eruption using ECHAM5 part 1: Sensitivity to the modes of atmospheric circulation and boundary conditions. *Atmospheric Chemistry and Physics*, *9*(2), 757–769. https://doi.org/10.5194/acp-9-757-2009

Thomason, L. W., Ernest, N., Millán, L., Rieger, L., Bourassa, A., & Vernier, J.-P. (2018). Peter, t. *A global space-based stratospheric aerosol climatology: 1979–2016. Earth System Science Data*, *10*(1), 469–492. https://doi.org/10.5194/essd-10-469-2018

Toohey, M., Krüger, K., Bittner, M., Timmreck, C., & Schmidt, H. (2014). The impact of volcanic aerosol on the Northern Hemisphere stratospheric polar vortex: Mechanisms and sensitivity to forcing structure. *Atmospheric Chemistry and Physics*, *14*(23), 13,063–13,079. https://doi.org/10.5194/acp-14-13063-2014

Toohey, M., Krger, K., Schmidt, H., Timmreck, C., Sigl, M., Stoffel, M., & Wilson, R. (2019). Disproportionately strong climate forcing from extratropical explosive volcanic eruptions. *Nature Geoscience*, *12*(2), 100–107. https://doi.org/10.1038/s41561-018-0286-2

Toohey, M., Stevens, B., Schmidt, H., & Timmreck, C. (2016). Easy volcanic aerosol (EVA v1.0): An idealized forcing generator for climate simulations. *Geoscien-tific Model Development*, *9*(11), 4049–4070. https://doi.org/10.5194/gmd-9-4049-2016

Vecchi, G. A., Delworth, T., Gudgel, R., Kapnick, S., Rosati, A., Wittenberg, A. T., & Zhang, S. (2014). On the seasonal forecasting of regional tropical cyclone activity. *Journal of Climate*, *27*(21), 7994–8016. https://doi.org/10.1175/jcli-d-14-00158.1

Vecchi, G. A., & Soden, B. J. (2007). Increased tropical Atlantic wind shear in model projections of global warming. *Geophysical Research Letters*, *34*, L08702. https://doi.org/10.1029/2006GL028905

Winton, M., Takahashi, K., & Held, I. M. (2010). Importance of ocean heat uptake efficacy to transient climate change. *Journal of Climate*, *23*(9), 2333–2344. https://doi.org/10.1175/2009jcli3139.1

Winton, M., Anderson, W. G., Delworth, T. L., Griffes, S. M., Hurlin, W. J., & Rosati, A. (2014). Has coarse ocean resolution biased simulations of transient climate sensitivity? *Geophysical Research Letters*, *41*, 8522–8529. https://doi.org/10.1002/2014gl061523

Wunderlich, F., & Mitchell, D. M. (2017). Revisiting the observed surface climate response to large volcanic eruptions. *Atmospheric Chemistry and Physics*, *17*(1), 485–499. https://doi.org/10.5194/acp-17-485-2017

Yan, Q., Zhang, Z., & Wang, H. (2018). Divergent responses of tropical cyclone genesis factors to strong volcanic eruptions at different latitudes. *Climate Dynamics*, *50*(5), 2121–2136. https://doi.org/10.1007/s00382-017-3739-1

Yang, X., Vecchi, G. A., Gudgel, R. G., Delworth, T. L., Zhang, S., & Rosati, A. (2015). Balaji, v. *Journal of Climate*, *28*(9), 3592–3611. https://doi.org/10.1175/jcli-d-14-00517.1

Zanchettin, D., Bothe, O., Graf, H. F., Lorenz, S. J., Luterbacher, J., Timmreck, C., & Jungclaus, J. H. (2013). Background conditions influence the decadal climate response to strong volcanic eruptions. *Journal of Geophysical Research: Atmospheres*, *118*, 4090–4106. https://doi.org/10.1002/jgrd.50229

Zanchettin, D., Khodri, M., Timmreck, C., Toohey, M., Schmidt, A., Gerber, E. P., & Tummon, F. (2016). The model intercomparison project on the climatic response to volcanic forcing (VolMIP): Experimental design and forcing input data for CMIP6. *Geoscientific Model Development*, *9*(8), 2701–2719. https://doi.org/10.5194/gmd-9-2701-2016

Zhang, W., Villarini, G., Vecchi, G. A., & Murakami, H. (2018). Impacts of the Pacific meridional mode on landfalling North Atlantic tropical cyclones. *Climate Dynamics*, *50*(3), 991–1006. https://doi.org/10.1007/s00382-017-3656-3

Zuo, M., Man, W., Zhou, T., & Guo, Z. (2018). Different impacts of northern, tropical, and southern volcanic eruptions on the tropical Pacific SST in the last millennium. *Journal of Climate*, *31*(17), 6729–6744. https://doi.org/10.1175/JCLI-D-17-0571.1